IJE TRANSACTIONS B: Applications Vol. 34, No. 05, (May 2021) 1145-1155

International Journal of Engineering

Journal Homepage: www.ije.ir

Large-scale Experimental Study on Collapsible Soil Improvement using Encased Stone Columns

M. Bahrami*, S. M. Marandi

Department of Civil Engineering, Shahid Bahonar University of Kerman, Kerman, Iran

PAPER INFO

Paper history:
Received 24 December 2020
Received in revised form 06 April 2021
Accepted 12 April 2021

Keywords:
Collapsible Soil
Large-scale Specimens
Stone Columns
Geogrid-encased
Aspect Ratio
Soil Improvement

ABSTRACT

The aim of this study was to improve the characteristics of natural collapsible soils using the geogrid-encased stone column technique. For this purpose, 20 large-scale specimens of stone columns were prepared using rigid metal cylinders with a diameter of 308 mm and a height of 97 to 154 mm according to the unit cell theory. The aspect ratio was 10 to 25%. For the occurrence of bulging failure, the height of the stone columns was considered six times the diameter. The stone columns were encased with geogrids of varying stiffness from 80 to 200 kN/m. The soil around the stone column inside the unit cell was compacted to similar site conditions. Loading was applied similar to the test, which determines the soil collapsibility potential while the specimens were being inundated from the bottom of the metal cylinder by a water feeding system. During loading, the vertical displacements of the stone columns were measured at two locations on the loading plate. The results showed that the columns settlement due to inundation diminished by increasing the stiffness of the encased stone columns and aspect ratio. The optimum aspect ratio was approximately 15%. Encasement of the stone columns increased the lateral pressure in the collapsible soil and prevented the collapse of the stone column. The settlement values of stone columns were compared with a settlement prediction model and showed a good agreement. The data obtained in this study can be used as a practical method to improve natural collapsible soils during inundation.

***doi**: 10.5829/ije.2021.34.05b.08*

1. INTRODUCTION

Collapsible soils are partially saturated deposits whose void ratio drastically diminishes by an unexpected increase in moisture content with or without additional loading. Such types of soils are problematic to practice in geotechnical engineering. They are usually found in silty clay deposits, sedimentary loess soils, sand dunes, and gypsum silt in both arid and semi-arid regions. If the collapsible soil underneath the any structural foundations is saturated, it will encounter a large settlement. The collapsibility settlement of soil is caused by the reduction of lateral support of the surrounding soil while it collapses. Thus, the identification and modification of these types of soils is necessary prior to construction of structures.

Researchers who have addressed the methods to identify collapsible soils or predicting their settlement during inundation have provided many reports [1-3]. A complex theoretical and practical mathematical model created in order to test how the operating system works after heavy and long rains when the soil moisture is greatly increase [4]. A research was carried out to quantify the permeability in micro-scale porous structures [5].

Other researchers have proposed different methods for improving the performance of collapsible soils. Engineered compacted fills may possess collapsible behavior [6, 7]. Soils compacted within certain specifications might experience considerable collapse as well [8].

Attempts have been made to stabilize problematic soils by means of chemical additives. For example, the

*Corresponding Author Institutional Email: bahrami@eng.uk.ac.ir (M.Bahrami)

Please cite this article as: M. Bahrami, S. M. Marandi, Large-scale Experimental Study on Collapsible Soil Improvement using Encased Stone Columns, International Journal of Engineering, Transactions B: Applications Vol. 34, No. 05, (2021) 1145-1155

effect of aerobic microorganisms on grain soil improvement in Garmsar industrial town was evaluated experimentally in order to investigate the effects of these phenomena on soil shear strength and stiffness [9]. The results showed that the unconfined compressive strength and stiffness of the soil increased by adding the microbial solution. Hosseini et al. [10] used electrokinetics and nanomaterials to stimulate the additives to move through soil pores, as an in-situ remedial measure. The results revealed that the collapse potential significantly improved by using 3% lime and 5% nanomaterial. A study explored the effect of three kinds of nanomaterial, including nano-silica (NS), nano-clay (NC) and nano-calcium carbonate (NCC) on the properties of a loessial collapsible soil [11]. The results showed that a small amount of nanomaterial (less than 1% of the total dry weight of the soil) could significantly improve the mechanical behavior of the loessial collapsible soil. An experimental study was performed to understand the effect of improving collapsible soil using polyethylene / Nano-lime mixture [12]. The results indicated that the improvement produced a significant change in the collapse potential, permeability, compressibility, and shear strength.

Houston and Houston [13] used pre-wetting as an improvement technique for the collapsible soil. Rollins and Rogers [14] performed the pre-wetting technique in conducting full-scale tests on wetted collapsible soil with 2% sodium silicate solution.

Use of geotextile and geogrid as reinforcement to improve bearing capacity and to reduce settlement for foundation on layered soils has also been examined. Ayadat [15] designed a physical model (390 mm inside diameter, 520 mm depth and 17.5 mm wall thickness) and implemented a geotextile-encased sand column. The collapsible soil used in this investigation was made in the laboratory by a mixture gap-graded soil. The mixture was made of 78% concrete sand, 10% Leighton buzzard sand (less than 90 μm), and 12% kaolin clay. Hanna and Solyman [16] designed an experimental prototype for testing rigid strips foundation on collapsible soils subjected to inundation due to raise of the groundwater table. Collapsible soils have been partially replaced with cohesionless materials with and without a geotextile reinforcing layer. They found a significant improvement in reducing the collapse settlement in the case of a combining of partially replaced collapsible soil with geotextile layer at the interface.

Several numerical studies have also examined the parametric effect of encased geotextile stiffness [17, 18]. Marandi et al. [19] as well as Alonso and Jimenez [20] analyzed the uncertainty and reliability of using stone columns. Demir and Sarici [21] in a laboratory work and numerical analysis explored the behavior of stone column with or without geogrid in clayey soil. Alkhorshid et al. [22] tested the performance of encased columns constructed on a very soft soil using three woven geotextiles and different column fill materials. The results showed that breakage of column filling materials would affect the load-settlement behavior of gravel and recycled waste columns.

A review of the existing literature showed that extensive numerical and experimental works have been performed on collapsible soil improvement; however, few studies have been reported on improving the use of natural collapsible soils with stone column techniques. Most researchers have prepared the collapsed soil in the laboratory by mixing sand and clay [15]. Preparation of artificial soil in the laboratory can affect soil cementation that exists in the natural soil deposition in the field. However, these studies did not lead to preparation of guidelines on the foundation analysis and design on collapsible soils. Thus, professional engineers are not sufficiently confident to design conventional foundations on collapsible soils. In addition, the majority of researchers have artificially produced collapsible soils in the laboratory by mixing sand and clay soils in their respective studies. On the other hand, one of the important reasons for the occurrence of collapse during inundation is the reduction of lateral pressure in the soil, so the technique of encased stone column is one of the most effective solutions.

Since the results of laboratory methods should be used in the field, it seems that the scale of the experimental study is of particular importance. This study sought to develop the stone column technique by conducting large-scale experiments near the field scale to find a solution to improve the collapsible soil. In this case, the results of large-scale experiments can be easily generalized to the field. Further, by setting up large-scale experiments, it is possible to provide the conditions under which materials can be used on a real scale.Thus, in the present work; large-scale experimental program was designed and implemented to improve the natural collapsible soils using encased stone columns with geogrid and crushed aggregate in order to develop new data for engineering earthworks.

2. MATERIALS AND METHODS

2. 1. Soil Properties and Characteristics The soil samples used in this research were collected from the southern part of a vast collapsible zone located in Kerman, Iran. To characterize the in-situ collapsible soil, 15 boreholes were drilled with depths of 10 to 30 m in the sampling region. The disturbed and undisturbed samples were prepared at varying depths of boreholes. The Standard Penetration Test (SPT), in-situ soil unit weight, natural water content, and soil electrical resistance tests were performed on the site. The results are shown in Table 1.

TABLE 1. In-situ soil characteristics

Characteristic	Value
SPT	19-26 blows/30 cm
Dry unit weight	13.10-14.40 kN/m^3
Natural water content	7.1-16.5 %
Electrical Resistance	1-5 Ω-m

In the laboratory, the analysis of the particle size, plasticity indices, specific gravity of solids, conventional undrained and drained triaxial, collapsibility potential, and soil chemical tests was carried out according to the standard methods of ASTM D422, ASTM D421, ASTM D854, BS 1377, ASTM D5333, and ASTM D1411, respectively. According to the Unified Soil Classification System (USCS), the soil classification in the site was generally in the CL soil group to the end of the depth of 30 m. The soil grading curves used in this study are shown in Figure 1. The physical, mechanical, and chemical properties of the soil are presented in Table 2.

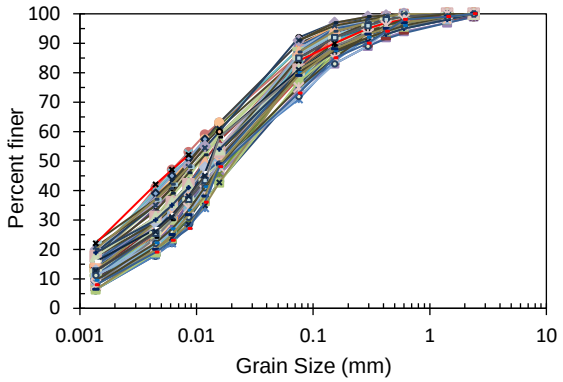

Figure 1. Grain size distribution of in-situ soil

TABLE 2. Soil physical, mechanical, and chemical properties

Property	Value
PI	8-12%
Activity Index	0.15-0.31%
Liquidity Index	-1.38 to -0.24
CP (Collapsibility potential)	2.0-5.7%
e_0 (initial void ratio)	0.790-0.910
Specific gravity of solids (GS)	2.529-2.548
Saturation Degree (S)	27-39%
c_u	30-60 kPa
c'	3.1-6.2 kPa
φ'	24-31 deg.
pH	8.2
SiO2	47%
CaO	17%
Sulphates in term of Ca SO4	1.6%
Chlorides in term of Cl-	0.03%

By considering the plasticity indices and the particle size finer than 2 microns, it was determined that the collected soil was inactive. The liquidity index shows that the soil was slightly over consolidated clay. Although the amount of collapsibility potential was low to moderate (2-5.7%), significant damage was observed at the site due to collapsibility. Further, the soil dispersive potential was investigated by determining sodium, potassium, calcium and magnesium ions. (Table 3). Based on the results of the chemical analysis, the dispersive potential of the soil used in this study is negligible.

In order to determine the effect of specimen disturbance factor on collapsibility potential (CP), the collapsibility potential tests were performed on a number of specimens consisting of remolded and undisturbed specimens. The results are presented in Table 4. The results revealed that the CP for the undisturbed specimens was slightly higher than that for the undisturbed specimens. This difference is due to the voids in remolded specimens, which have more uniform distribution than in the undisturbed specimens. Thus, more voids are exposed to soak during inundation.

2. 2. Characteristics of Crushed Aggregate The uniform aggregates used to construct the stone columns were prepared from angular limestone chips with a nominal size ranging from 9 to 25 mm. The sieve analysis of crushed aggregate is demonstrated in Figure 2. The scale of the unit cell was so large that these crushed materials were used inside the stone column on their actual scale.

The minimum and maximum densities of the crushed stone were determined using standard tests of ASTM D4253 and ASTM D4254, respectively. Based on ASTM D3080, the internal friction angle of crushed stone was measured by a large direct shear box under vertical stresses of 100, 200, and 300 kPa. The specimens were prepared with the maximum unit weight of crushed aggregate. The characteristics of crushed aggregate are presented in Table 5.

TABLE 3. Soil chemical analysis for dispersive potential

EC (ms/cm)	Na^+ (meq/L)	K^+ (meq/L)	Ca^{++} (meq/L)	Mg^{++} (meq/L)
3-6	8.5-15.5	0.18-0.41	5.1-11.6	0.4-4.3

TABLE 4. CP of remolded and undisturbed specimens

Types of specimen	γ_d (kN/m^3)	Water content (%)	S (%)	e_0	CP (%)
Un-disturbed	14.1-14.3	6.8-8.5	22-28	0.781-0.797	3.8-4.4
Remolded	13.9-14.2	7.1-9.2	26-30	0.792-.818	5.1-5.9

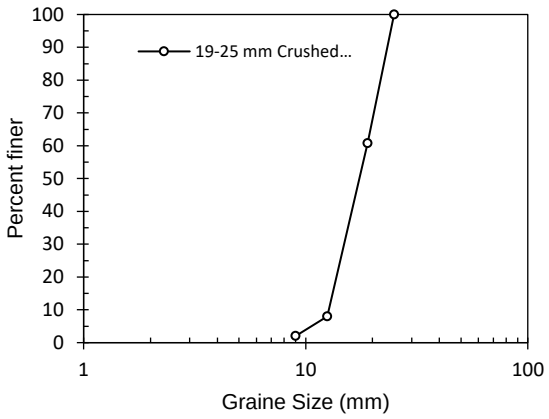

Figure 2. Grain size distribution of crushed stone

TABLE 5. Crushed aggregate characteristics

Characteristic	Value
USCS	GP
Maximum unit weight	15.3 kN/m^3
Minimum unit weight	13.5 kN/m^3
φ'	44 deg.

2. 3. Geogrid Characteristics In the present research, three types of commercial named For Tex uni-axial geogrid were used to encase the stone columns. The geogrids were manufactured by weaving polyester micro yarns in a rectangular format and were coated with PVC. According to the manufacturer, the technical specifications of geogrids, adapted from Istanbul Teknik Corporation, are shown in Table 6. MD and CMD stand for machine direction cross machine direction, respectively.

2. 4. Design of Laboratory Testing Program for Stone Column Models For designing the stone columns models, the experimental program was considered the unit cell concept with 308 mm in diameter and triangular pattern in the field. The diameters of the stone columns were calculated with respect to the desired aspect ratios (Ar.) in the designed program. The testing program for the stone column model is shown in Table 7. Further, two models were designed for individual soil (S0) and soil with non-encased stone column (SC).

The L/D ratio (length to diameter of the stone column) was used five for the single stone column in the experimental studies. Ghazavi and Nazari Afshar [23] showed that at least L/D = 4 is required to control the bulging failure mode. In this study, in order to overcome the bulging failure mode of the stone columns, the height of each specimen was chosen to be six times greater than its diameter.

2. 5. Design and Manufacturing Accessories The loading device and accessories were designed to model the implementation of the stone column replacement method. The loading system capable of stress control method was made of steel. The device rig included a hydraulic jack with capacity of 600 kN by installing a 100 kN load measurement dial gauge. The front and planar views of the large-scale loading frame are shown in Figure 3.

To manufacture the unit cell tanks, a seamless Mannesmann metal tube was prepared with 12 m in length, 305 mm internal diameter, and 10 mm in thickness. Four tanks with heights of 900 to 1200 mm were cut from the Mannesmann metal tube. After turning and polishing, the inner tanks' diameter was 308 mm. The base plates with 450 mm in diameter and 25 mm in thickness were welded to the bottom of these tanks. At the central of the base plate, a threaded metal rod with a height of 50 mm was installed to provide space for filter materials. A brass lattice plate was designed to be screwed to the metal rod in the base plate at the height of the filter material. Around the perimeter of the brass plate, a semicircular groove was designed to sit an O-ring, which could seal the tank wall entirely. Three water ducts of 10 mm in diameter were created across the base plate to allow water to seep into the tank from its outside. To control the flow rate, three faucets measuring 6 mm in diameters were placed on the water pipe paths in the tank exterior.

TABLE 6. Technical characteristics of the geogrids

Type of geogrid	Tensile Strength (kN/m)		Elongation in Nominal Strength (%)	
	MD	CMD	MD	CMD
ForTex GG 80/30 P	80	30	12(±2)	12(±2)
ForTex GG 120/30 P	120	30	12(±2)	12(±2)
ForTex GG 200/50 P	200	50	12(±2)	12(±2)

TABLE 7. Testing program for the stone column models

Model type		SC1	SC2	SC3	SC4
Ar (%)	Aspect ratio	10	15	20	25
D_e (mm)	Unit cell diameter	308	308	308	308
$D = D_e\sqrt{A_r}$ (mm)	Stone column diameter	97.4	119.3	137.7	154.0
L (mm)	Stone column height	584	716	826	924

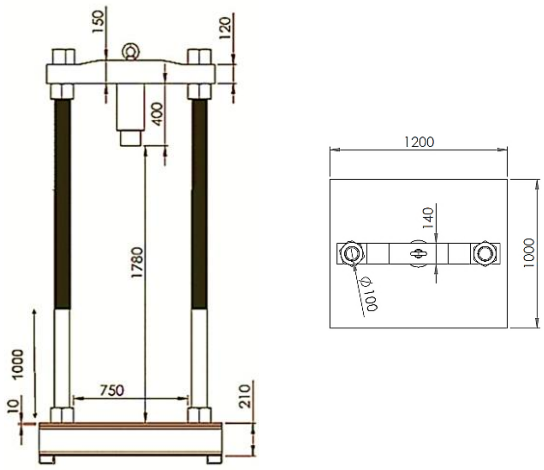

(a) (b)

Figure 3. Large-scale loading frame (a) Front, (b) Planar view

Four steel thin-walled tubes with 800 mm in height, 2 mm in thickness, and the outer diameters equal to the diameters of the stone columns were designed for developing the stone columns model. At the bottom of the drainage brass plate, four circular grooves (2 mm wide) were made to place the stone columns vertically inside the unit cell tank.

To compact the soil around the stone column, two light compaction hammers were welded to each other at a distance proportional to the diameter of the unit cell.

To inundate the specimens, a water-flow system was selected from the bottom to the top of the tank. An 80-L water barrel was placed on a four-legged metal base at altitude of 2 m above the laboratory floor. A glass box was prepared with dimensions of 20 cm × 20 cm × 30 cm for creating a laminar and steady state flow of water. At the upper side of this box, two valves with 19 and 6 mm in diameters were embedded for water inlet and air outlet, respectively. Three valves with 6 mm in diameters were installed on three vertical sides of the glass box. Silicone hoses were installed to allow water to flow from the glass box to the valves mounted in the outer part of the tank base plate. Figure 4 illustrates the test rig set up of the large-scale experimental model.

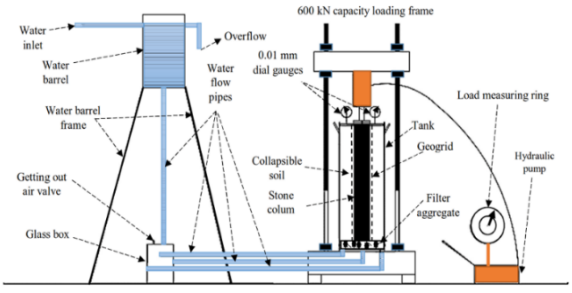

Figure 4. The test rig setup

2. 6. Test Procedure To minimize the skin friction, the inner wall of the unit cell tank was covered with a thin layer of grease. The filtering material was placed in the tank bottom up to a height of 50 mm. The drainage brass plate was screwed about 5 mm to the metal rod of the tank bottom. The geogrid was wrapped around the stone column models and fixed by sewing with polymer yarn. The geogrid-encased tube was placed inside the tank in the prepared groove at the bottom of the brass lattice plate. The tank was prepared to place the soil around the stone columns.

For each tank, about 80 kg of dried soil, passed through a 4.75 mm sieve, and was mixed with water (8.5% by weight of water content) as a homogeneous mixture. The soil mixture was stored for 24 h in a container with no change in its moisture content. Then, the required quantity of wet soil was weighed according to the wet unit weight of the soil with respect to 50 mm height of the tank. The soil was slowly placed around the stone column model tube inside the tank. The compacting device was inserted into the tank. In this way, the compaction hammers was placed on the top of the hollow plate. Then the compaction hammers were pulled up with a rope where impact energy was introduced for attaining the predicted value of the height of the soil within the tank.

The weighed crushed aggregate to build a height of 50 mm of the stone column was placed into the tube and vibrated by an electrical vibrator hose until the desired height was attained. Finally, the sand between 8 and 16 mesh sieves was used to smooth and level the surface of the stone column. In this way, specimens were prepared. Figure 5 shows the tank setup and prepared specimens SC1 and SC4, respectively.

The specimens were transferred to the loading device lifted using ceiling crane and forklift. The specimen was adjusted at its place in the center of the loading device. Three hoses from the outlet valves of the dividing glass box were connected to the three valves inlets at the bottom base plate of the tank. Then, all valves were closed. A 15 mm thick steel plate with the same

Figure 5. Prepared specimens SC1 and SC4

diameter of stone column was placed on top of the specimens. The specimen was prepared for loading. In order to apply the load axially, a special metallic connector was used between the loading piston and the loading plate. Two vertical displacement gauges were connected and aligned to the loading plate using the magnetic connector (Figure 6).

Loading was carried out according to the collapsibility potential test standard. Stresses of 25, 50, 100, and 200 kPa were applied in conditions where the specimen had a natural moisture content. A constant stress of 200 kPa was applied for 24 h. After this period, the three water valves were opened to allow the water to flow into the drainage system and inundate the specimen. During the experiment, the water head was kept constant. Then 400, 800, 1600 and 3200 kPa stresses were applied to the inundated specimen. The loading steps were carried out according to the stress control method and the vertical displacement gauge readings were recorded until they stopped. At the end of the experiments, the inundated specimens were taken from the laboratory and disposed of in a suitable place away from any contamination in the environment.

2. 7. Repeatability of Tests After preparing the collapsible soils and assembling the rig, a number of preliminary tests were conducted to verify the repeatability of the tests. Equation 1 was used to determine the repeatability based on the BS 812 standard.

$$r_1 = 2.8\sqrt{V_r} \quad (1)$$

where V_r represents the repeatability variance and r_1 denotes the value of repeatability, below which the absolute difference of the results of two single test may be expected to lie with a probability of 95%. The displacement values above the stone column for the three iterations with Ar. = 15 % under 200 kPa stress were 11.23, 12.01, and 11.83 mm, respectively. The repeatability variance was 0.17 and $r_1 = 1.14$. The maximum absolute difference value between 12.01 and 11.23 was 0.78, which was smaller than the previous repeatability value; thus, the test results have been acceptable when it comes to repeatability.

Figure 6. Prepared specimen for loading

3. RESULTS AND DISCUSIONS

3. 1. Results The stress-settlement tests results are shown in Figure 7 which are related to soil settlement alone (S0, the specimen without stone column and geogrid) and non-encased stone columns (SC, stone column without geogrid) specimens. Comparison between two series of the settlement curves shows that the non-encased stone column has not significantly reduced the settlement caused by the inundation in the collapsible soil. When water enters the specimen, the soil structure collapses, and the crushed aggregate particles of the stone column, which are not lateral protected, also collapse. Thus, the presence of a stone column without lateral support does not have the ability to improve collapsible soil behavior and reduce the collapsibility settlement.

Figure 8 displays the variations of stress versus settlement of stone columns without geogrid and encased geogrids with various stiffness. It can be observed that there is a significant difference between the vertical displacements of the non-encased and geogrid-encased stone columns. Further, the collapsible soil volume decreases suddenly and the lateral pressure is induced when the soil is inundated. However, if the stone column is encased with reinforcing elements, the lack of lateral pressure surrounding the stone column is prevented. Thus, the geogrid-encased stone column has more load-bearing capacity and reduces suddenly settlement of surrounding soil.

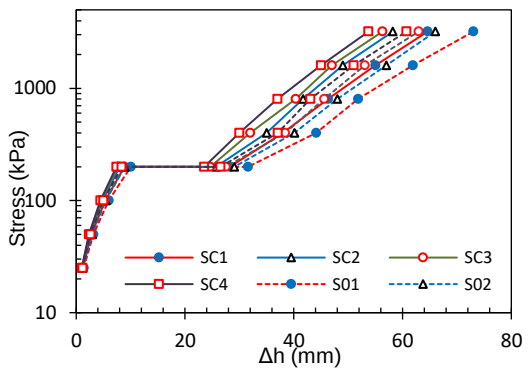

Figure 7. Variations of stress versus vertical displacement of soil alone and uncased stone columns

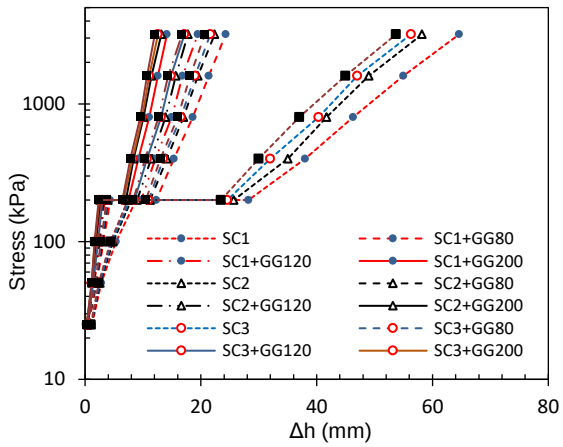

Figure 8. Stress versus vertical displacement with different conditions of stone columns

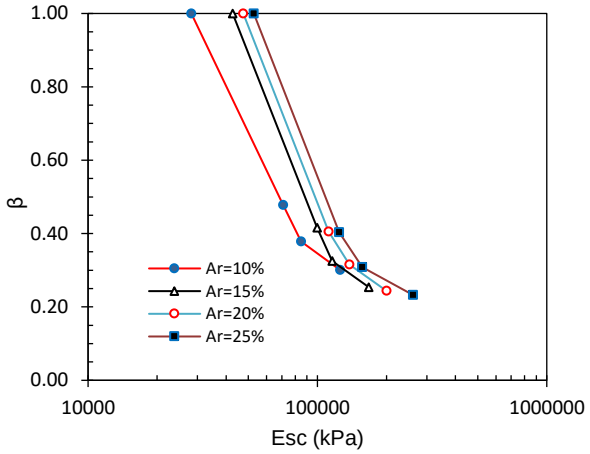

Figure 9. Changes of β versus Esc

3. 2. Data Analysis To analyze the settlement reduction factor for various experimental models, the variations in settlement reduction factor versus deformation modulus of the stone columns are used for different aspect ratios. The factor of reduction (β), presented by Ayadat and Hanna [35], was introduced in accordance with Equation (2):

$$\beta = \frac{S_i}{S_0} \quad (2)$$

where, Si denotes the stone column settlement and S0 represents the settlement of uncased column.

After inundating the specimens, the slope of stress-displacement curves for encased stone column was slightly higher than the slope of stone column without encasement. This is due to an increase in lateral pressure by the geogrid. There was no obvious difference between slopes of stress-displacement curves with increase in geogrid stiffness. Thus, increasing the geogrid stiffness as a constraining factor did not play a significant role in the settlement reduction factor.

As shown in Figure 9, the settlement reduction factor, β, has decreased following the increased stiffness of the stone column (Esc) or increased aspect ratio, Ar. The elastic modulus of the stone columns was calculated from the slope of the straight-line stress-deformation curves beyond inundation. With increase in the aspect ratio and the stiffness of the stone column, the vertical settlement diminished after inundation and the factor of β dropped in respect to Equation (2). Interestingly, the vertical settlement of the stone column was greatly influenced by the settlement brought about through its lateral displacement.

An increase in the elastic modulus of the stone column, the settlement caused by the lateral deformation can be increased to a certain value. The gentle slope at the end of the curves occurs frequently in the modulus of elasticity, with the rate of settlement reduction factor being low.

Figure 10 manifests the variations of settlement reduction factor against geogrid stiffness for various stone column aspect ratios. The results revealed that the settlement reduction factor diminished with all aspect ratios. With increasing aspect ratio, the crushed aggregate has replaced instead of soil. In this case, the elasticity modulus of the stone column increased and as a result, the stone column settlement diminished. Further, the results showed that the curve of Ar. = 15% was significantly different from the other curves, which were not significantly different among each other. Thus, the optimal aspect ratio was about 15%. This conclusion is in agreement with what was found in Figure 10 with a significant difference in the vertical settlement between the SC1 and SC2 curves.

The stone column technique can easily generalize the laboratory results to the practical scale in the field. Using the optimal aspect ratio Ar. =15% and the relationships (Equations 3 to 6) between the elements of the stone column [24], the actual diameter in the field can be calculated for triangular and square patterns of stone columns.

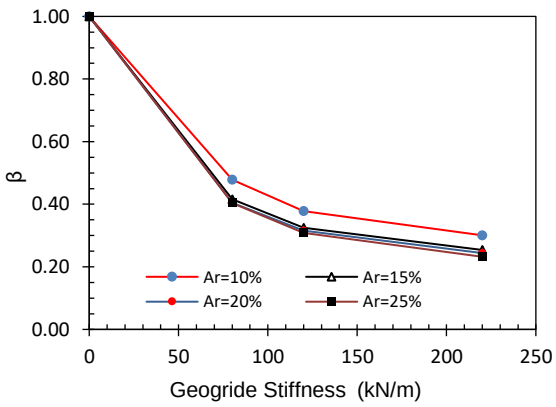

Figure 10. Variations of β versus geogrid stiffness

$$D_e = 1.05 \times S \quad (3)$$

$$D_e = 1.13 \times S \quad (4)$$

$$A_r = \frac{A_s}{A} \quad (5)$$

$$D = D_e \times \sqrt{A_r} \quad (6)$$

where, Equations (3) and (4) belong to triangular and square patterns, respectively; S is axis-to-axis distance between two adjacent rows of the stone columns; A_s is the area of stone column; A represents the unit cell area.

Typically, the diameter of the column is selected and the distance between two rows of columns in the desired pattern is calculated based on the optimal aspect ratio. In nature, there are thick layers of collapsible soil that have considerable resistance, but if they get too wet, they lose their strength, whereby extensive settlement and lateral deformation occur. By significantly reducing the vertical displacement of stone columns encased with geogrids in the collapsible soil as a modifier, this system can provide the conditions for safe transfer of the structure loads to the ground at depth

Based on Equation (7) the ratio of the stone column settlement to the collapsible layer thickness determines the collapsibility potential (CP).

$$CP = \frac{\Delta H}{H_0} \quad (7)$$

where, ΔH denotes the soil settlement with or without the stone column; and H_0 represents the collapsible soil thickness. Figure 11 shows the variations of collapsibility potential versus stone column stiffness under various Ar. and full inundation. The results also show that with increase in the aspect ratio and the stone column stiffness the CP drops significantly. The major decline in the CP reflects the role of the confinement of stone columns. From Figure 11, it can be calculated that at the 15% aspect ratio, the amount of collapsibility potential is reduced by about 82%.

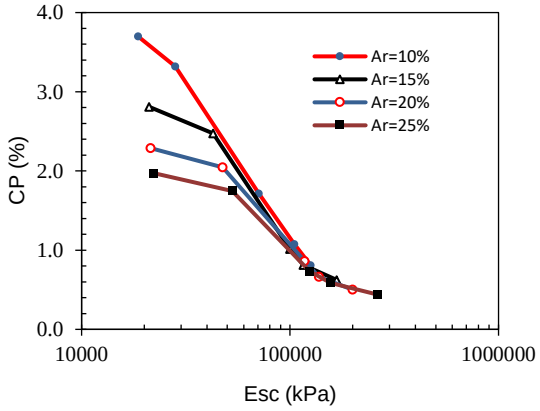

Figure 11. Changes of collapsibility potential versus Esc

3. 3. Analytical Model for Settlement Analysis

Since the settlement of stone columns was the most widely discussed matter, the intention of the analytical model was considered to predict the settlement. The settlement of the inundated stone column, which is completely penetrated into the collapsible soil and is subjected to the external axial stress of σ_a, consists of three constituents.

$$\Delta = \sum_1^3 \delta_i \quad (8)$$

where, Δ is the sum of settlement caused by the stone column inundation forced by the external load of P; δ_1 is the stone column elastic displacement brought by the stress leading to inundation; δ_2 represents the settlement caused by the downward pulling force due to the consolidated surrounding soil of the stone column; δ_3 denotes the vertical settlement caused by the stone column lateral movement.

$$\delta_1 = \frac{\sigma_a L}{E_{sc}} \quad (9)$$

$$\delta_2 = \frac{2\sigma_a L^2}{E_{sc} d}\left[C' + K_0 tan\varphi'\left(\frac{\gamma L}{3\sigma_a} + 1\right)\right] Q_R Q_T \quad (10)$$

where, σ_a is the stress at which inundation occurs, E_{sc} shows the elastic modulus, L denotes the height, d indicates the stone column diameter (d = $2r_0$), C' shows the soil adhesion under drainage conditions, φ' shows the internal friction angle of the soil under drained condition, δ_2 is the axial displacement of the stone column during failure. Q_R and Q_T are correction factors for cases when full stone column–soil skid does not occur, and the delayed effects in the installation stone column, respectively [25].

The resistance of stone column against lateral pressure is boosted by adding of the geogrid materials in comparison with the soil alone. When the geogrid is subjected to tensile stress, it applies an additional pressure onto the column, and further aids the reinforcement. Using the tensile strength of the geogrid materials (τ) this pressure can be calculated. Figure 12 reveals the cylindrical specimen of geogrid associated with the lateral pressure Δσ.

The third component of Δ is presented as follows [26]:

$$\delta_3 = 2\Delta P \frac{r_0 L}{Et} \quad (11)$$

where E is the elastic modulus of the cylinder encasing the column, and

$$\Delta P = \sigma'_V K_{as} - \sigma'_r \quad (12)$$

$$K_{as} = tan^2\left(\frac{\pi}{4} - \frac{\varphi'}{2}\right) \quad (13)$$

where, σ'_v is the vertical stress exerted on the column and σ'_r denotes the effective lateral pressure applied on the column peripherally. Thus, the total settlement is defined as follows:

$$\Delta = \frac{\sigma_a L}{E_{sc}} + \frac{2\sigma_a L^2}{E_{sc} d}\left[C' + K_0 tan\varphi'\left(\frac{\gamma L}{3\sigma_a} + 1\right)\right] Q_R Q_T + 2\Delta P \frac{r_0 L}{Et} \quad (14)$$

The comparison of the measured values in the large-scale experimental study and predicted models for β, on top of the stone column due to column inundated under a given condition of stress (200 kPa) is as shown in Figure 13. It can be observed that there is a sufficient correlation between the values, especially as regards to the percentages that are lower than the aspect ratio between the predicted and measured experimental values. The results of the present study showed that the new experimental data and model behavior are in agreement with what was found by other researchers such as Ayadat and Hanna [26].

The obtained data in this study may be used as an applied method for improving the natural collapsible soil during inundation using encased stone columns.

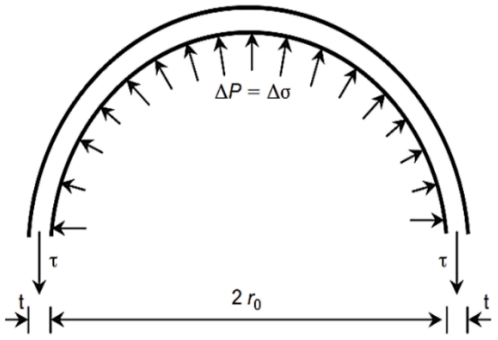

Figure 12. Cylindrical specimen of geogrid against the lateral pressure Δσ

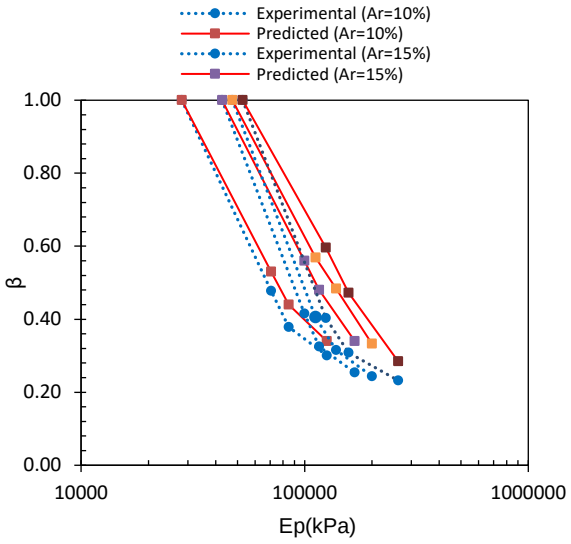

Figure 13. Variations of the settlement reduction factor along with the Esc

4. COCLUSIONS

A Large-scale experimental study was performed on collapsible soil improvement using geogrid-encased stone columns and the following results were achieved:

1. The implementation of the stone column without geogrid had no effect on the settlement reduction factor in collapsible soil under inundation conditions. The use of stone columns without lateral support in the collapsible soil during inundation caused premature failure of the stone column.
2. The optimal aspect ratio in encased stone column with geogrid was obtained as approximately 15%. In this case, the collapsibility potential was reduced by 82%.
3. The stone column technique can easily generalize the laboratory results to the practical scale in the field. Using the geometric relationships between the elements of the stone columns in different patterns and the optimal aspect ratio obtained from this study, the large-scale laboratory results could be easily generalized to the scale in the field.
4. The encasement of the stone column with geogrid increased the lateral pressure in the collapsible soil where the settlement due to the collapsibility was drastically reduced.
5. By significantly reducing the vertical displacement of stone columns encased with geogrids in the collapsible soil, this system can provide the conditions for safe transfer of the structure loads to the depth.
6. Increasing the geogrid stiffness as a confining support did not play a significant role in the settlement reduction factor in collapsible soil.
7. The experimental results on encapsulated stone columns were predicted well using the theoretical approach for settlement calculation.

By setting up large-scale experiments, it is possible to provide the conditions under which materials can be used on a real scale. The scale of the unit cell was so large that the crushed materials were used inside the stone column in their actual scale. In this case, the actual behavior and performance of the materials were demonstrated. It is necessary to implement the stone column technique in collapsible soil with an aspect ratio of 15% in the field to gain feedback on the behavior of the system on full scale.

5. REFERENCES

1. Pereira, J. F.H., and Fredlund, D.G., "Volume change behavior of collapsible compacted gneiss soil", ***Journal Geotechnical and Geoenvironmental Engineering***, Vol. 126, No. 10, (2000), 907-916. doi: 10.1061/(ASCE)1090-0241(2000)126:10(907).
2. Gaaver, Kh. E., "Geotechnical properties of Egyptian collapsible soils", ***Alexandria Engineering Journal***, Vol. 51, No. 3, (2012), 205-210. doi:10.1016/j.aej.2012.05.002.
3. Ayadat, T. and Hanna, A. M., "Assessment of soil collapse prediction methods", ***International Journal of Engineering,***

Transactions B: Applications, Vol. 25, No. 1, (2012), 19-26. doi:10.5829/idosi.ije.2012.25.01b.03.

4. Mihajlovic, G., Zivkovic, M., "Sieving Extremely Wet Earth Mass by Means of Oscillatory Transporting Platform ", ***Emerging Science Journal,*** Vol. 4, No. 3, (2020), 172-182. doi: 10.28991/esj-2020-01221.
5. Fazelabdolabadi, B., Golestan, M. H., "Towards Bayesian Quantification of Permeability in Micro-scale Porous Structures – The Database of Micro Networks", ***HighTech and Innovation Journal,*** Vol. 1, No. 4, (2020), 148-160. doi: 10.28991/HIJ-2020-01-04-02.
6. Ishihara, K., and Harada, K, "Cyclic behavior of partially saturated collapsible soils subjected to water permeation" ***Ground failures under seismic***, No. 44, (1994), 34-50.
7. Houston, S. L., Houston, W. N., Zapata, C. E., and Lawrence, C., "Geotechnical engineering practice for collapsible soils" ***Journal of Geotechnical and Geological Engineering***, No. 19, (2001), 333-355. doi: 10.1023/ A: 1013178 226615.
8. Lim, Y.Y. and Miller, G. A., "Wetting-induced compression of compacted Oklahoma soils" ***Geotechnical and Geoenvironmental Engineering***, Vol. 130, No. 10, (2004), 1014-1023. doi: 10.1061/(ASCE) 1090-0241(2004) 130:10 (1014).
9. Jalili, M., Ghasemi, M. R., Pifloush, A. R., "Stiffness and Strength of Granular Soils Improved by Biological Treatment Bacteria Microbial Cements", ***Emerging Science Journal***, Vol. 2, No. 4, (2018), 219-227. doi: 10.28991/esj-2018-01146.
10. Hosseini, A., Haeri, S. M., Siavash Mahvelati, S., Fathi, A., "Feasibility of using electrokinetics and nanomaterials to stabilize and improve collapsible soils", ***Journal of Rock Mechanics and Geotechnical Engineering***, Vol. 11, No. 5, (2019), 1055-1065. doi: 10.1016/j.jrmge. 2019.06.004.
11. Haeri, M., Valishzadeh, A., "Evaluation of Using Different Nanomaterials to Stabilize the Collapsible Loessial Soil", ***International Journal of Civil Engineering***, No. 156, (2020). doi: 10.1007/s40999-020-00583-9.
12. Margherita, Z., Laura, E., Chiara, M. M., Roberto, S., Bartolomeo, M., "Collapsible intact soil stabilisation using non-aqueous polymeric vehicle", ***Engineering Geology***, Vol. 264, (2020), 105334. doi: 10.1016/j.enggeo. 2019.105334
13. Houston, W. N. and Houston, S. L., "State of the practice: Mitigation measures for collapsible soil sites", ***Foundation Engineering***, Current Principles and Practices, Evanston, IL, USA, (1989), 161-175.
14. Rollins, K. M. and Rogers, G. W., "Mitigation measures for small structures on collapsible alluvial soils" ***Journal of Geotechnical Engineering***, Vol. 120, No. 9, (1994), 1533-1553. doi: 10.1061/(ASCE)0733-9410(1994)120:9(1533).
15. Ayadat, T., "Collapse of stone column foundations due to inundation", Ph.D. Thesis, Sheffield University, Sheffield, United Kingdom, (1990).
16. Hanna, A., Soliman, S., "Experimental Investigation of Foundation on Collapsible Soils", ***Journal of Geotechnical and Geoenvironmental Engineering***, Vol. 143, No. 11, (2017), 1-12. doi: 10.1061/(ASCE)GT.1943-5606.0001750.
17. Almeida, M.S.S., Hosseinpour, I., Riccio, M., "Performance of a geosynthetic encased column (GEC) in soft ground: numerical and analytical studies", ***Geosynthetics International***, Vol. 20, No. 4, (2013), 252-262. doi: 10.1680/gein. 13.00015.
18. Murugesan, S., Rajagopal, K., "Geosynthetic-encased stone columns: numerical evaluation", ***Geotextiles and Geomembranes***, Vol. 24, No. 6, (2007), 349-358. doi: 10.1016 /j.geotexmem.2006.05.001.
19. Marandi, S.M., Anvar, M. and Bahrami, M., "Uncertainty analysis of safety factor of embankment built on stone column improved soft soil using fuzzy logic α cut technique", ***Computers and Geotechnics***, Vol. 75, No. 5, (2016), 135-144. doi: 10.1016/ j.compgeo.2016.01.014.
20. Alonso, J., Jimenez, R., "Reliability-based design of stone columns for ground improvement considering two settlement failure modes" The XVI European Conference on Soil Mechanics and Geotechnical Engineering: Geotechnical Engineering for Infrastructure and Development, Edinburgh, Scotland, November, (2015).
21. Demir, A., Sarici. T., "Bearing capacity of footing supported by geogrid encased stone columns on soft soil", ***Geomechanics and Engineering***, Vol. 12, No. 3, (2017), 417-439. doi:10.12989/gae.2017.12.3.417.
22. Alkhorshid, N.R., Araujo, P.L.S., Palmeira, E.M., Zornberg, J.G., "Large-scale load capacity tests on a geosynthetic encased column", ***Geotextiles and Geomembranes***, Vol. 47, No. 5, (2019), 632-641. doi:10.1016/j.geotexmem. 2019.103458.
23. Ghazavi, M., Nazariafshar, J., "Bearing Capacity of Geosynthetic Encased Stone Columns, ***Geotextiles and Geomembranes***, Vol. 38, No. 6, (2013), 26-36. doi: 10.1016/j.geotexmem. 2013.04.003.
24. Barksdale, R.D., Bachus, R. C., "Design and construction of stone columns, Federal High way administration Office of Engineering and Highway Operations Research and Development, FHWA/RD-83/029", School of Civil Engineering, Georgia, Georgia, UAS, (1983).
25. Poulos, H. G., Davis, E. R., *Pile Foundation Analysis and Design*, John Wiley & Sons, New York. N.Y., USA, (1980).
26. Ayadat, T., Hanna, A. M., "Encapsulated stone columns as a soil improvement technique for collapsible soil", ***Ground Improvement***, Vol. 9, No. 4, (2005), 137-147. doi: 10.1980/grim. 2005.9.4.137.

Persian Abstract

چکیده

هدف از این مطالعه، بهبود خصوصیات خاک‌های فروریزشی طبیعی با استفاده از تکنیک ستون‌سنگی دورپیچی‌شده با ژئوگرید بود. برای این منظور ۲۰ نمونه بزرگ مقیاس از ستون سنگی بر اساس نظریه سلول واحد با استفاده استوانه‌های فلزی صلب به قطر ۳۰۸ میلی‌متر و ارتفاع ۹۷ تا ۱۵۴ میلی‌متر ساخته‌شدند. نسبت سطح ستون سنگی به سلول واحد از ۱۰٪ تا ۲۵٪ تغییرداده‌شد. برای رخداد شکست شکم‌دادگی، ارتفاع ستون‌های سنگی شش برابر قطر درنظرگرفته‌شد. لوله‌های فلزی مدل ستون‌های سنگی با ژئوگریدهایی دارای سختی‌های متفاوت از ۸۰ تا ۲۰۰ کیلونیوتن بر متر دورپیچی و درون استوانه‌های سلول واحد قرارداده‌شدند. در داخل این لوله‌ها مصالح سنگی شکسته و اطراف آن خاک رمبنده با شرایط محل اجراشد. بارگذاری شبیه به روش آزمایش تعیین قابلیت فروریزشی خاک، در حالی اعمال‌شد که نمونه از پایین استوانه فلزی به وسیله یک سیستم بالاآوردن سطح آب در حال غرقاب‌شدن بود. در اثنای بارگذاری، جابجایی‌های قائم ستون‌ها در دو محل روی صفحه بارگذاری اندازه‌گیری‌گردید. نتایج نشان‌داد که با افزایش سختی ستون‌های سنگی محصورشده و نسبت سطح، باعث کاهش نشست آن‌ها در اثر غرقاب‌شدگی شد. بهینه نسبت سطح ستون‌های سنگی تقریباً ۱۵٪ بدست‌آمد. دورپیچی ستون‌های سنگی باعث افزایش فشارجانبی در خاک شد و از فروریختن ناگهانی ستون سنگی جلوگیری‌کرد. مقادیر نشست اندازه‌گیری‌شده از نتایج آزمایشگاهی با خروجی نتایج یک مدل تحلیلی محاسبه‌شد. مقایسه نتایج اندازه‌گیری‌شده و مدل محاسباتی، مطابقت خوبی را نشان‌داد. داده‌های به دست‌آمده در این مطالعه می‌تواند به عنوان یک روش کاربردی برای بهبود خاک فروریزشی طبیعی در هنگام غرقاب‌شدگی مورد استفاده عملی قرارگیرند.